Field emission characterization of field-aligned carbon nanotubes synthesized in an environmental transmission electron microscope

Pascal Vincent, Federico Panciera, Ileana Florea, Anthony Ayari, Sorin Perisanu, Costel Sorin Cojocaru, Haifa Taoum, Chen Wei, Khakimjon Saidov, Utkur Mirsaidov, et al.

J. Vac. Sci. Technol. B 42, 022802 (2024) https://doi.org/10.1116/6.0003413

Field Emission characterization of field-aligned carbon nanotubes synthesised in an Environmental Transmission Electron Microscope

Pascal Vincent,[1, a)] Federico Panciera,[2, a)] Ileana Florea,[3, b)] Anthony Ayari,[1] Sorin Perisanu,[1] Costel Sorin Cojocaru,[3] Haifa Taoum,[3] Chen Wei,[2] Khakimjon Saidov,[4] Utkur Mirsaidov,[4] Ilias Aguili,[1] Nicholas Blanchard,[1] Pierre Legagneux,[5] and Stephen Thomas Purcell[1]

[1)] *Univ Lyon, Univ Claude Bernard Lyon 1, CNRS, Institut Lumière Matière, F-69622, Villeurbanne, France.*

[2)] *Université Paris-Saclay, CNRS, Centre for Nanoscience and Nanotechnology, 91120 Palaiseau, France.*

[3)] *Laboratory of Physics of Interfaces and Thin Films, UMR CNRS 7647, Ecole Polytechnique, IP-Paris, 91228 Palaiseau, France.*

[4)] *Centre for BioImaging Sciences, Departments of Physics and Biological Sciences, National University of Singapore, 14 Science Drive 4, Singapore 117557.*

[5)] *Thales Research and Technology, 91767 Palaiseau, France.*

(*Electronic mail: if@crhea.cnrs.fr)

(*Electronic mail: federico.panciera@c2n.upsaclay.fr)

(*Electronic mail: pascal.vincent@univ-lyon1.fr)

(Dated: 15 February 2024)

Optimizing the synthesis of carbon nanotubes (CNTs) for applications like Field Emission (FE) sources requires a fundamental understanding of the growth kinetics of individual CNTs. In this article, we explore how applying electric fields during CNT synthesis influences the as-grown nanotubes and their FE performance. We observe growth and undertake FE measurements in real time using an environmental transmission electron microscope. This is achieved through a polarizable capacitor gap within a microchip sample heater specifically designed for this purpose. Individual nanotubes are easily resolved and are predominantly single-wall CNTs. At low-applied fields, the growing nanotubes can span the gap and link with the opposite electrode, albeit with some loss due to mechanical failure. With a high-applied field and positive bias for FE, we continue to observe the oriented growth of nanotubes. However, this growth is constrained within the gap due to the possibility of FE occurring during the growth process, which can result in either saturation or damage. At any given time, we have the flexibility to halt the growth process and conduct *in situ* FE experiments. This approach enables us to comprehensively track the complete development of the CNTs and gain insights into the various mechanisms responsible for limiting the performance of CNT cathodes. Interestingly, we report an original self oscillation induced destruction mechanism that has not been reported before.

I. INTRODUCTION

Owing to their unique properties, carbon nanotubes (CNTs), although discovered three decades ago, are still being actively investigated as electron field emission (FE) sources for a number of applications[1] including space propulsion systems[2], X-ray generation[3] and X-ray tomography[4,5], high brightness electron guns for microscopy[6] and microwave amplifiers[7,8].

To improve the performance of planar nanotube cathodes various preparation techniques ranging from direct synthesis to nanotube shaping have been tested (see for example[9] and[10]). Whatever the production method, the FE performances of CNT cathodes are primarily tested through current-voltage I(V) characterization where microscopic observation of the individual nanotubes is not possible. This makes it difficult to understand precisely the measured variations and to interpret the I(V)s.

On the other hand, more fundamental studies have focused on the direct observation of individual nanotubes during FE in electron microscopes (SEM and TEM) or by Field Emission Microscopy (FEM) for a better understanding of the various limiting mechanisms and in order to be able to optimize the CNTs performance. These works have for example highlighted the phenomena of gradual destruction by evaporation[11–13] or by mechanical tearing[14] as well as the determination of the maximum currents that can be obtained per nanotube, typically between 200 nA and 2 μA[15] for single wall nanotubes (SWNTs). However, these experiments were performed on relatively few nanotubes and the samples used are often very different from the classical planar cathode structures.

An interesting approach would be to bring together these different configurations to simultaneously observe a large number of nanotubes in a planar geometry from the synthesis stage, then the first I(V) measurements and finally the different limiting and destructive mechanisms.

This article describes our recently achieved breakthrough on the dynamical observation of Electric Field Directed Synthesis (EFDS)[16] and FE of carbon nanotubes using micromachined chip heaters in Environmental Transmission and Scanning Electron Microscopes (ETEM and SEM). A key in-

[a)] Corresponding authors

[b)] Corresponding authors; current adress : Université Cote d'Azur, CNRS, CRHEA, 06 905 Sophia Antipolis cedex, France.

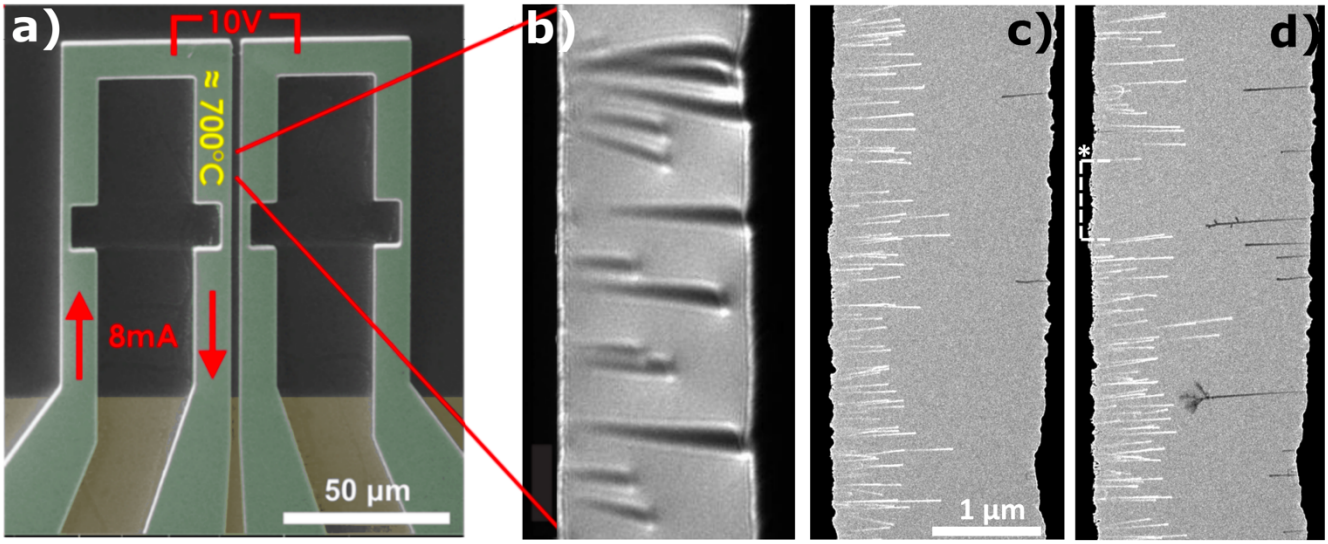

FIG. 1. Experimental setup used for *in situ* EFDS of SWNTs and FE experiments in an Environmental Transmission Electron Microscope. a) SEM image of the active zone of the micro-machined chip heater with two close cantilevers. One cantilever is heated by the Joule effect and a polarising voltage is applied between the two cantilevers. Growth is observed across the gap where the electric field is maximum. b) TEM observation during a 'low voltage regime' synthesis (see text). We observe nanotubes (visible as black lines) crossing the gap and attached to the opposite electrode. c) and d) Observations during a 'high voltage regime' synthesis (50 V). The two images correspond to 81 s and 156 s after growth starts. Nanotubes appear here as bright lines. No nanotube crosses the gap due to ultimately FE related mechanisms that limit the length of nanotubes. In d) black lines connected on the other side, named nanodarts, are observed, corresponding to torn-off carbon nanotubes that have crashed onto the opposite electrode. The white dotted segment under the asterisk corresponds to a simultaneous destruction zone discussed in the text. Note that the contrast in the images depends on the TEM settings used for imaging and the applied voltages.

novative aspect is that applied electric fields direct the systematic fabrication of extremely straight and preferentially single-wall carbon nanotubes (SWNTs). Depending on the applied electric field strength and polarity FE may occur during the synthesis. Under appropriate conditions large FE currents are obtainable that can ultimately limit the growth of the SWNTs due to field-induced evaporation. An unexpected and notable aspect of these experiments was the observation of numerous nanotubes torn from the synthesis electrode and finally firmly connected to the opposite electrode (so called 'nanodarts'), forming potentially interesting nano-objects for FE applications. Results obtained on the EFDS of SWNTs (orientation, growth rates, growth rate variation, etc.) have recently been published[16]. In this paper we focus more specifically on the different FE related mechanisms during synthesis and FE measurements realized post-synthesis. These direct observations provide unique insights into the evolution of nanotubes during I(V) measurements and a better understanding of the destruction mechanisms such as gradual destruction, mechanical rupture and a novel self-oscillation induced destruction mechanism observed during our experiments.

In the following the experimental system and the main aspects of growth in an electric field are first described with a particular emphasis on the FE phenomena and the destruction mechanisms. The formation and evolution of "nanodarts" is also discussed. We then focus on FE measurements and I(V)s performed after synthesis. These observations enable us to track the nanotubes' evolution during the measurements and to witness various destruction mechanisms, including the one driven by self-oscillations. Finally, current densities obtained during our experiments are discussed.

II. EXPERIMENTAL SETUP AND SYNTHESIS UNDER ELECTRIC FIELD

A. Experimental setup

The CNT growth experiments under the influence of an *in situ* electric field, along with FE experiments, are conducted using specially designed microchips that can be mounted on a Protochips Fusion sample holder. These chips enable simultaneous heating and polarization of the sample. A SEM image of the active part of the micro-chip is presented in Fig. 1 a) where one can observe the two close free-standing cantilevers separated by a 2 μm gap with their electric connections. The *in situ* real time TEM observations were performed using a modified environmental transmission electron microscope (Titan ETEM 60-300ST) operated at 80 keV.

Samples are prepared according to the following procedure (more details are presented in[16]). The cantilevers are first covered by a 5 nm alumina layer and 0.7 nm Fe thin layer in a high precision ultra-high vacuum molecular beam evaporator. Both layers are deposited at room temperature directly on the cantilevers. The role of the alumina during the growth process is to allow the formation of nanometric Fe clusters by Oswald ripening while preventing their fast migration. The microchip is then transferred into the TEM column and one of

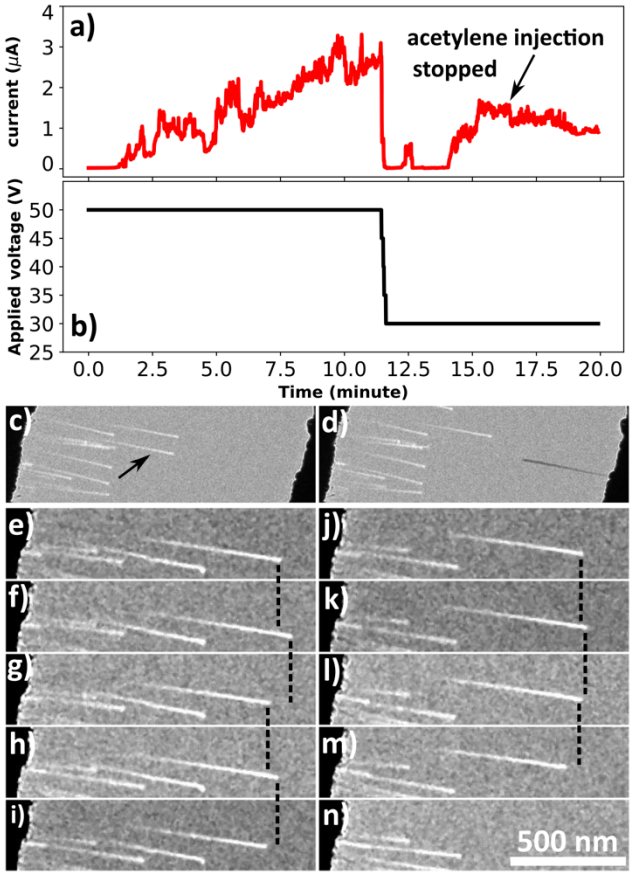

FIG. 2. a) and b) Field emission current and applied voltage evolutions during the synthesis corresponding to images Fig. 1 c) and d). The voltage was first set to 50 V and then reduced to 30 V at the end. At 50 V the global emission current increased to 3 μA before the voltage drop. c) and d) Successive images during the growth showing an example of formation of a nanodart. The arrow in c) indicates the nanotube that has been torn-off and then forms the black nanodart in the next frame. e) to n) Evolution of the length of a growing nanotube that is simultaneously field evaporated at the apex. Successive length increases and reductions are observed that are the result of the competition between growth and evaporation. In n) the nanotube is finally destroyed.

the two cantilevers was selected to be heated by the Joule effect for a preliminary hydrogen pre-treatment of the catalyst. An electrometer is connected to the counter electrode to control its bias and measure the FE current. For growth, acetylene (C_2H_2) is used as carbon feedstock mixed with H_2. This gas mixture is introduced into the chamber and once the pressure is stabilized the cantilever temperature is slowly increased until roughly 650-700 °C in the growth zone. As nanotubes begin to grow the video recording (at 4 frames per second) is started.

A non-trivial aspect concerns the nanotube contrast in the videos. To make nanotubes visible during growth in this low magnification observation mode, the image-forming lens is intentionally defocused (underfocused or overfocused). The contrast thus depends mainly on two parameters: the applied polarisation and the defocusing. For a given polarization and defocus, nanotubes either appear bright or dark. Altering either the defocus or polarization flips the contrast, transforming a bright nanotube into a dark one, and vice versa. The nanotubes are single-walled, regardless of their contrast. The difference in contrast for example between Fig. 1 b) and c) corresponds to two different defocus settings (positive voltage applied to the counter electrode so FE is possible). It's worth noting that when the applied voltage is too low, the nanotubes cannot be observed. After each synthesis HRTEM observations are made. These observations clearly prove a "base-growth" mechanism and confirm that nanotubes are essentially SWNTs. Typical diameter distributions of the synthesized SWNTs show a mean diameter of around 1 nm.[16]

B. Low / High voltage regime

We conducted syntheses at various biases. The majority of the syntheses were carried out using positive bias applied to the counter-electrode (FE possible) with potential differences between 4 V to 50 V. For comparison, some growths using negative polarization were also performed, the electrostatic forces being identical but without field emission. Very good alignment is observed for all tested voltages. Depending on the applied voltage, two regimes can be distinguished for the synthesis depending on whether the nanotubes can reach the opposite electrode or not. For the "low voltage regime" (approximately less than 20 V) some nanotubes disappear during the growth (probably due to being mechanically torn out of the electrode by the electrostatic force) but the majority reach the counter electrode. A number of nanotubes are destroyed during the contact, which seems to depend on the applied potential difference, while the others adhere. As the synthesis proceeds, more and more nanotubes are observed crossing the gap and some stick together (by Van der Waals forces) forming Y shapes and small bundles in the center of the gap. An example of "low voltage" growth is shown in Fig. 1 b) where several nanotubes connected to the two electrodes are visible. It may seem surprising that the nanotubes are not systematically destroyed during the contact with the counter electrode for voltages greater than 10 V. This is probably due to the very high contact resistance that can exist between the nanotube and the silicon based cantilever (the barrier layer is composed of 5 nm of alumina). For classical FE where electrons are emitted in vacuum, FE is possible only for voltage difference higher than the work function, typically 4.5-5 eV. For higher voltages it is possible that some nanotubes emit electrons during the synthesis. However, in this case the electron emission does not lead to the apparent destruction of the tubes.

At higher positive biases a significantly different growth regime is observed ("high voltage regime"). A movie of the first 3 minutes growth under high polarization (50 V) is provided in the Supplementary materials (SM-video1[17]). In this case the nanotubes appear as bright segments that grow perpendicular to the electrodes. Two images corresponding to 81 and 156 s of the synthesis are presented in Fig. 1 c) and d). In the video many nanotubes growing simultaneously per-

J. Vac. Sci. Technol. B 42, 022802 (2024) https://doi.org/10.1116/6.0003413

pendicular to the gap are distinguishable. However a large number suddenly disappear and very few reach 2/3 of the gap. The majority appear to barely reach the middle of the gap. Similarly, although new nanotubes grow regularly, in Fig. 1 d), taken 1 minute later, an increase in nanotube density is not observed, confirming their continual destruction. At high voltage and negative bias (no field emission), we also observe many nanotubes disappearing but a few of them can reach the opposite electrode where they are destroyed upon contact. This indicates that in positive polarization it is ultimately the field emission mechanism that limits the growth of nanotubes in the gap. The applied voltage as well as the emission current were recorded during the synthesis and are presented in Fig. 2 a) and b). At the beginning of the growth, where the voltage is 50 V, one observes a progressive current increase up to about 3 μA (note that during all the experiments the pressure was of the order of 10^{-4} mbar which is a poor vacuum for field emission and explains the very noisy measured current). Note that increased length at fixed voltage leads automatically to linearly increasing apex electric field and thus exponentially increased FE current. A last proof of the length limitation by the FE process is that during the same synthesis the voltage was reduced from 50 to 30 V and the nanotubes growing with the lower applied voltage grew longer and nearly reached the opposite electrode.

C. Destruction mechanisms during growth

During nanotube growth three types of destruction mechanisms have been identified. In the first the totality of a nanotube disappears from the image due to mechanical ripping-off at their bases by the electrostatic forces. This ripping-off of whole CNTs is confirmed by an appreciable fraction of these disappearances being immediately followed by the appearance of a black line on the opposite region of the counter electrode. An illustration is presented in Fig. 2 c) and d) which shows two consecutive frames of the same area. The nanotube indicated by the black arrow in c) has disappeared while in d) a black line has simultaneously appeared on the opposite electrode. The most likely mechanism is that the torn-off nanotube, which is charged, is accelerated by the field and then sticks to the opposite electrode. If the tube binds firmly to the electrode it will then become positively charged and aligned by the field like the nanotubes on the heated electrode. Due to the TEM settings used to enhance contrast the nanotube appears black in the image. We term these objects "nanodarts". In some cases, very rare in our observations, the disappearance of a part of a tube is followed by the appearance of a black line on the opposite electrode. This shows that in some cases the nanotubes may break at a defect. In the destruction mechanism leading to the total disappearance of the nanotubes it seems that the contact between the nanotube and the sample (interface between barrier layer and catalyst or catalyst/nanotube) is too weak to resist the electrostatic forces.

In a second type of destruction process during synthesis, the length of some nanotubes successively increases and decreases, a phenomenon interpreted as field evaporation that is thermally activated by field emission. (see Fig. 2 e) to n)). This mechanism of gradual destruction has been clearly demonstrated for SWNTs by Dean, *et al.*[11] In this mechanism the strong current emitted by the nanotube leads to a significant temperature rise at the tip (more than 1600 K estimated in[11] and temperatures up to 2000 K have been measured by electron spectroscopy[13]). The high field combined with the temperature can then lead to field evaporation that shortens

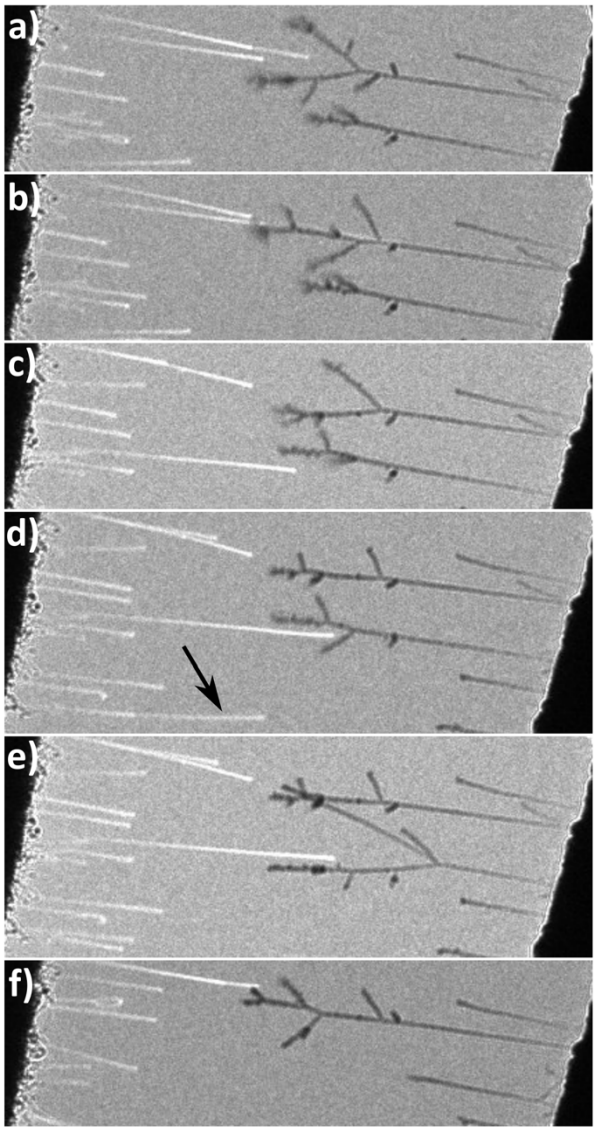

FIG. 3. a) to f) Evolution in time of different nanodarts.The two longest nanodarts seem to show a dendritic growth. In fact, these nanodarts electrostatically attract the debris torn-off from the growth electrode and form new branches. These branches, more or less robust, repel each other electrostatically. Images d) and e) correspond to two consecutive frames in the video. In e) a new long branch appear on the lower nanodart that correspond at the simultaneous disappearance of a long nanotube on the opposite electrode (see black arrow in d)) indicating that this tube has been attracted and connected to the nanodart.

the SWNT and therefore moderates the field emission current and the heating. Elegant observations of this phenomenon by TEM on individual nanotubes have been done by Wang *et al.*[12] Here this mechanism occurs during the synthesis and the evolution of the length of the nanotube results from the combined effect of the synthesis and the evaporation. Other examples of the evaporation mechanism during synthesis are provided in[16]. It is remarkable that this field evaporation mechanism, which requires high current, field and temperature at the free end, is concomitant with the synthesis of the nanotube at the opposing end. As these high currents are indicative of strong electrostatic forces, these nanotubes also prove that robust mechanical connections between the support and the nanotubes are possible. Finally for all the cases clearly identified, this competition between evaporation and growth led to the complete disappearance of the nanotubes which seems to indicate the fragile equilibrium of this particular state.

The two previous mechanisms involved individual nanotubes. A third mechanism observed from time to time corresponds to the simultaneous disappearance of several nanotubes or even of a small region of the sample. An example can be seen in Fig. 1 d) where one can observe an absence of nanotubes a little above the middle of the image (delimited by the white dotted line and the asterisk). The origin of these simultaneous destruction events is not yet completely clear.

D. Nanodarts

Now examine more closely the nanodarts which constitute an intriguing and unexpected feature of growth with an applied electric field. They can be formed both during and after growth when field emission experiments are performed.

The first point concerns the firm attachment of the nanodarts to the opposite electrode. As they are attached to the positive electrode, electron emission is impossible, but they are subject to electrostatic forces. This raises the question of the bonding mechanism between the nanodart and the support. A first hypothesis is that a certain length of the nanotube lies on the substrate held by adhesion (Van der Waals interaction) while the visible vertical length is aligned in the gap by the electric field. This configuration is however unstable in the case of a flat and uniform surface and cannot persist: either adhesion dominates and the entire tube sticks to the substrate or the electrostatic force dominates and causes the part in contact with the substrate to detach.

To understand why the adhesion hypothesis is unstable it is interesting to compare our configuration with Atomic Force Microscopy (AFM) experiments carried out to determine the adhesion energy of SWNTs on clean and flat surfaces[18,19]. In these experiments a SWNT is stuck at the apex of a AFM cantilever and this cantilever is brought close to the surface so that a part of the nanotube adheres to the surface. Adhesion to the surface, for a 1D object as SWNT, is classically characterized by an adhesion energy per unit length in J/m. This adhesion energy per unit length has also the dimension of a force and can be expressed in Newton and viewed as an adhesion force. This is similar to "surface tension" for fluids that can be seen equivalently as an energy per unit area (in J/m^2) or as a force per unit length (in N/m). For example adhesion energy of 1.24 ± 0.11 $nJ.m^{-1}$ (nN) has been measured between SWNTs and clean silicon. At its other end the nanotube is subjected to the pulling force of the cantilever, which is proportional to the deflection of the lever. If the lever pulling force is less than the adhesion force, the system spontaneously lowers its potential energy by sticking an additional part of the nanotube to the substrate. This reduction in the suspended length of the nanotube causes an additional deflection of the lever and an increase of the pulling force. This process continues until the pulling force of the lever is exactly equal to the adhesion force of the nanotube. This results in an equilibrium position (which allows the adhesion energy to be measured) that is stable. When subjected to a perturbation, the system spontaneously returns to the equilibrium position.

At first sight this configuration is very similar with the electrostatic force playing the role of the pulling force. When the electrostatic force equals the adhesion force we have an equilibrium position. However, this equilibrium is unstable. Let's assume a perturbation consisting of a length of the nanotube detaching from the surface. The increase in the vertical part leads to an increase in the field amplification factor and therefore in the electric field at the apex and ultimately in the electrostatic force (for the AFM lever it would result in a decrease of pulling force). As this electrostatic force has become greater than the adhesion force, an additional part of the tube detaches, further increasing the electrostatic force. This results in the complete detachment of the nanotube. The same reasoning can be applied if we start by considering the bonding of a small additional part of the nanotube, which ultimately leads to the bonding of the entire nanotube. As previously stated no stable configuration can be obtained with adhesion and electrostatic forces for flat and uniform surfaces.

Finally, in the absence of electric field all the nanotubes should lie entirely parallel to the surface due to adhesion. However, when the voltage is temporarily reduced down to zero (no electric field) before being raised again, the nanodarts are still present. Therefore, the most likely hypothesis is that strong chemical bonds are created between the nanotube and the electrode during the impact. From an energetic point of view, let us consider for example a tube with a net charge of 100 e that has been ripped off the opposite electrode without any change of charge. Subjected to a potential difference of 50 V, the kinetic energy of the nanotube during the impact is 5 keV. This energy is relatively low and cannot cause the total fragmentation or atomization of the nanotube (C=C bond energy: 6.375 eV/bond). However, this energy is perhaps capable of strongly modifying the chemical arrangement at the site of impact. Upon impact of the nanodart with the silicon electrode, one can imagine the creation of very strong Si-C bonds. A deeper understanding of this mechanism requires further experimental studies coupled with numerical simulations.

We observe the loss of significantly more nanotubes than nanodarts being formed, which raises the question of what happens to the remaining nanotubes. It is likely that the majority of the nanotubes stick to the electrode along their length.

Another possibility is that a tube reaches the electrode but creates only a weak bond. In this case when it becomes positively charged the electrostatic forces dominate and it can be ripped off the anode electrode again and accelerated in the other direction to bombard the growth electrode where it can destroy nearby nanotubes. Thus a possible explanation for the simultaneous disappearance of several nanotubes on small areas discussed previously is a back bombardment due to a nanotube being ripped off the opposite electrode. This mechanism is too fast to be discerned in the films. The simplest estimates give sub μs inter electrode travel times for complete CNTs. If this mechanism is correct, the mechanical strength at the base is all the more important to obtain robust cathodes because it limits simultaneously the ripping-off of the tubes from their support and the back bombardment.

These nanodarts can also evolve considerably over time and form dendrite structures. It is important to note that the counter electrode is not heated and synthesis is impossible on this side. Fig. 3 illustrates the evolution over time of several close nanodarts. The two longest ones evolve by the addition and disappearance of branches. Images d) and e), which are two successive video frames, show the very rapid addition of a long branch on the lower nanodart. This addition is simultaneous with the disappearance of a long nanotube on the opposite electrode and it is likely that this long torn-off nanotube has stuck on the nanodart. It seems that these structures are formed because the nanodarts modify the field structure in the gap and attract the different charged pieces torn off on the first electrode leading to an apparently dendritic growth. Again, in this scenario, it is not clear how the bonds between the different parts of the agglomerated tubes are formed. We finally get 'Frankenstein'-like structures formed by many different nanotube parts and the electrostatic repulsion between the different branches causes the dendritic aspect.

The longest nanodarts can also interact via electrostatic attraction with the nanotubes growing from the opposite electrode. In the case of a nanotube and a nanodart in close proximity their mutual interactions can be intricate especially if the nanotube is emitting electrons. This can result in complex phenomena and we often observe in these cases vibrations or oscillations that are difficult to interpret.

It is worth noting that the formation of these nanodarts and their interaction with the growing nanotubes can be easily observed because the gap is only two microns wide. One may ask for example how these objects would evolve if the gap were wider at constant macroscopic electric field in the gap and, in a more general way, under which experimental conditions these nanodarts are formed as a function of voltage, kinetic energy, etc.

III. AFTER GROWTH OBSERVATIONS AND FE CHARACTERIZATION

A. First I(V)s after growth

Coming back to the synthesis presented in SM-video1, the growth was finally stopped by closing the acetylene supply to prepare post-growth FE measurements. Note that the heating and hydrogen had not been stopped.

For applications an important question that arises is : will the alignment of the nanotubes, due to electrostatic forces, be preserved if the voltage is reduced to 0 V as would be done, for example, to remove the cathode from the growth equipment and place it in a FE setup? To answer this question we set the voltage to zero before performing the first I(V) measurement.

Images of the sample at the end of synthesis and at the beginning of the first I(V), after reducing the voltage to zero, are given in Fig. 4 a) and b). The images at low applied voltage lack contrast, making it impossible to observe changes in nanotubes under such conditions. In Fig. 4 b) a noticeable reduction of the aligned CNTs is observed. Image analysis shows that nearly 60 % of the nanotubes are still present in the observed area. Observations realized on several samples show that on average 50% of the nanotubes remained aligned after the first voltage drop. Some of the missing nanotubes have evidently merged together, forming loops (see * in Fig. 4 b)), while others have likely adhered to the substrate, possibly in a way that inhibits their realignment via the electric field.

A particular case is the nanotube labelled "1" in Fig. 4 b) which curiously lengthened. In fact, the synthesis was stopped by closing the acetylene gas valve while the sample was still hot and the CNT continued to grow slightly because of the gas supply remaining beyond the valve.

A first I(V) measurement of up to 50 V, compared to the end of growth with 30 V applied (see Fig. 2), has been performed simultaneously with video recording. The video captured during the I(V) with the embedded I-V curve is given in SM-video2[17]. It allows the variations observed in the field emission current to be linked to the evolution of the nanotubes. Figures 4 b) and c) present images at the beginning and the end of the first I(V) and Fig. 5 a) and b) present the first I(V) and the corresponding "Fowler-Nordheim" (FN) curves. The solid black line corresponds to the increasing voltage part of the I(V) and the dotted red line to the decreasing part. Evolution of the emission current during the voltage increase is very irregular with plateaus and jumps. Interestingly the video allows us to understand some of these features. In Fig. 5 a) the first interesting point (labelled "1") is the plateau one can observe between 24 and 33 V at nearly 200 nA. It clearly corresponds in the video to the gradual destruction of the longest nanotube labelled "1" in Fig. 4 b). The rapid current increase afterwards may be due to the loop opening that results in another available nanotube for FE. In the video one observes that this nanotube is finally also gradually evaporated. The first abrupt drop of 500 nA (labelled "2" in Fig. 5 a)) is concomitant to a novel self-oscillation induced destruction of the tube labelled "2" in Fig. 4 b) (even if this happened almost in the same time as a partial breakage of the tube "1"). More precisely the field emitting nanotube starts to self oscillate and suddenly totally disappears (see discussion below). The second important drop ($\sim$550 nA, labelled "3" in Fig. 5 a)) does not correspond to a noticeable modification in the observed area. It is probably due to another tube destruction in another area of the cathode out of the field of view. Finally the de-

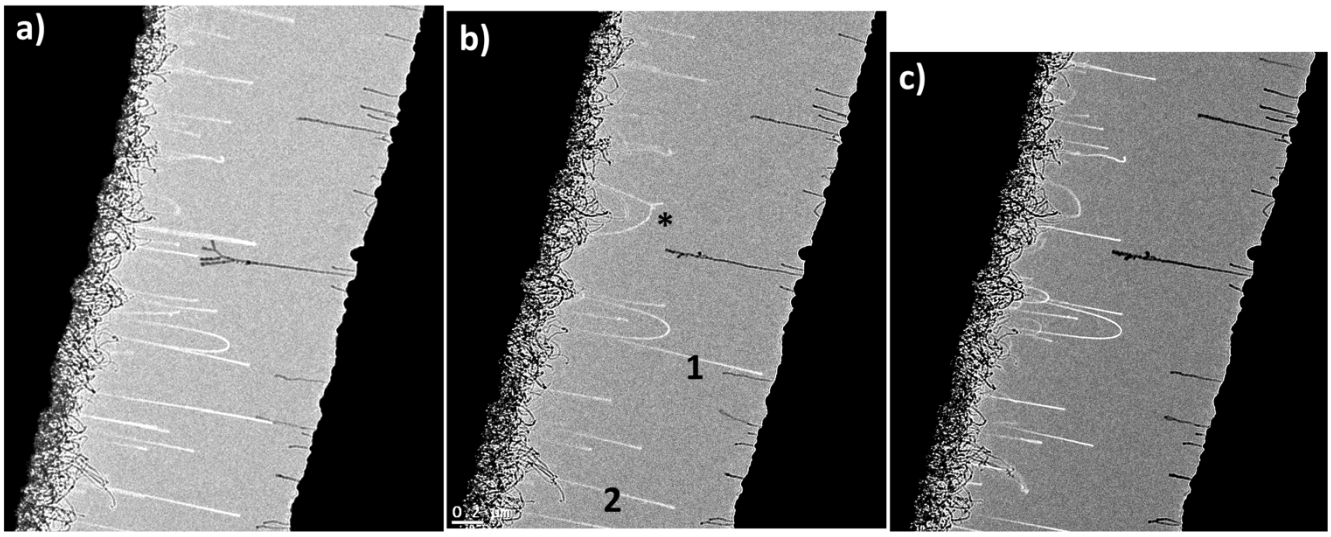

FIG. 4. Nanotube evolution between different experimental stages. a) Image of the cathode at the end of the synthesis after stopping the acetylene supply. b) Image of the cathode after a voltage reset and before the first I(V) measurement. We see that the number of aligned nanotubes has decreased. Nanotubes denoted 1, 2 and * are discussed in the text. c) Image of the sample after the first I(V) at 50 V.

creasing part of the I(V) is very smooth and follows a quasi metallic behaviour as can be seen by the straight line obtained in the Fowler-Nordheim representation in Fig. 5 b) and logically no evolution is observable in the video. The field and FE have removed the fragile CNTs.

The same procedure was repeated with the zero voltage setting before an identical I(V) measurement up to 50 V (see Fig. 5 c) and d)). The evolution is clearly smoother with only one noticeable apparent saturation indicated by an arrow. Final current at 50 V is slightly lower than in the first I(V) (1.9 μA instead of 2.5 μA) probably due to a additional small modification revealed by the saturation effect. Recording a video was not possible during this I(V) so we have no direct observation of the cause of this saturation. However, the emission current follows very closely the decreasing part of the first I(V). The FN curves of the second I(V) with the decreasing part of the first I(V) (in circle blue points) are plotted in Fig. 5 d). The curves are nearly identical meaning that the emitting nanotubes preserved after the first voltage drop are almost all preserved after the second voltage drop.

Examining the progression of the nanodarts in figures 4 a), b), and c), it is evident that they have mostly remained unchanged following the voltage drop and were not modified during the first I(V). To assess their FE performance, an I(V) test was conducted under reversed polarization conditions, reaching up to -50 V. I(V) curves obtained are shown in Fig. 5 e) and f) and appear to be very similar to the first I(V) in normal polarisation with an irregular increasing part with several jumps and a smooth decreasing part following a quasi metallic behavior. Interestingly the maximum current at -50 V is 1.75 μA, slightly inferior but of the same order as the emission of the nanotubes on the other electrode although their density is clearly lower. This raises the question of the interest of these nanodarts for FE cathodes. The sample in its entirety can also be seen as an ambipolar FE cathode as can be seen in 5 g) where we plotted the decreasing part of the I(V)s in normal and reversed polarisation. This configuration could be interesting for applications such as ambipolar gas discharge tubes[20,21] providing surge protection or for passive neutralization between different charged elements.

It should be noted that the strong field emission currents obtained under reverse polarization are clearly explained by the existence of nanodarts. Without these observations, or in another system, these emission currents would have seemed surprising not to say incomprehensible. In fact, one of the authors had previously measured notable emission currents in reverse polarization on nano-objects but had no explanation. The nanodarts or their equivalent likely explain those unexpected currents as well as the measurements presented here.

With this sample, we performed a lengthy synthesis (over 15 minutes) that was probably too long to produce an interesting cathode for field emission. Comparing the images in Fig. 1 c) and Fig. 4 a) it is clear that it would have been more interesting to stop the synthesis after about 2 minutes. In the first case a higher density of fine nanotubes is observed. Moreover, as the synthesis progresses, a kind of foam composed of large nanotubes and carbonaceous species develops on the surface of the sample, which probably hinders the growth of the following SWNTs. The presence of too many nanodarts also complicates the studies by modifying the behavior of the nanotubes on the opposite electrode. Consequently a shorter synthesis has been performed and is presented in Fig. 6 a). As expected no foam of large nanotubes is observed at the base and only one nanodart is visible. The nanotube density is however lower than in the first sample.

No I(V) curve has been performed with this sample but instead the voltage was changed over time and the field emission current was recorded simultaneously. The applied voltage and current evolution are presented in Fig. 7. Figures 6 b) and c) correspond to images of the sample after the first rise to 125

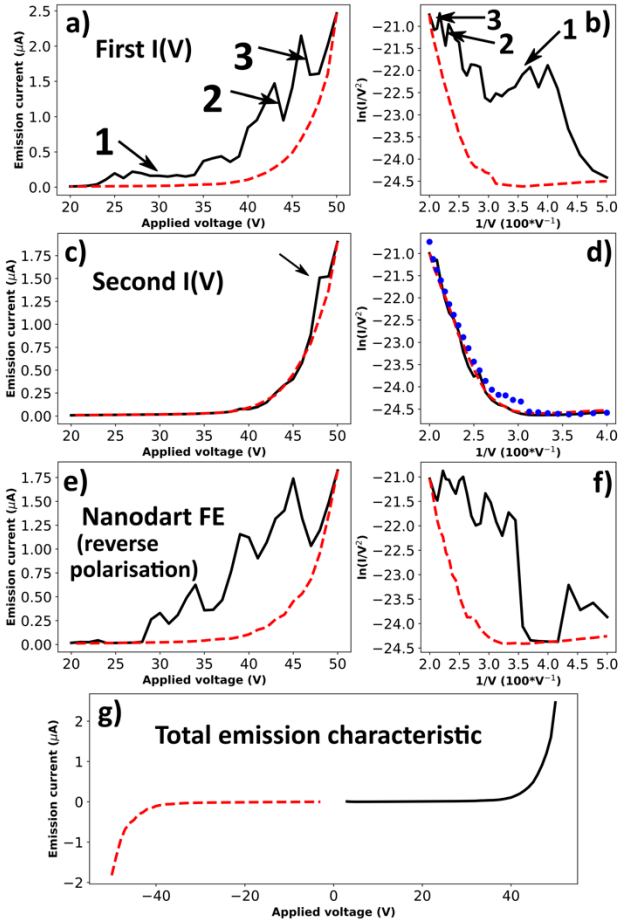

FIG. 5. a) First I(V) measurement after stopping the synthesis. The black solid line (respectively red dotted line) corresponds to the increasing part of I(V) (respectively decreasing). The areas indicated "1", "2" and "3" correspond respectively to a first plateau at 200 nA and to two important falls of the current. b) "Fowler-Nordheim" representation of the first I(V). c) Second I(V) measurement under the same conditions d) "Fowler-Nordheim" representation of the second I(V). e) I(V) realized in reversed bias corresponding to the field emission of the nanodarts. f) "Fowler-Nordheim" representation of the I(V) in reversed bias. g) Superposition of the I(V)s in normal and reversed bias showing that the cathode behaves like an almost symmetrical ambipolar diode.

V (4 μA) and after the application of the maximum voltage of 225 Volt (maximum current: 27.8 μA). In Fig. 7 b) these two moments are indicated by arrows. Following the application of 125 V (as shown in figure 6 b)), it is observed that all the longest nanotubes have either undergone significant shortening or have completely vanished. Also note the appearance of multiple nanodarts which clearly appeared during FE. These nanodarts can therefore be formed during both synthesis and field emission. These nanodarts seem also to protrude farther into the gap than the as grown nanotubes. Dashed lines in Fig. 6 b) show the average extent of nanotubes and nanodarts respectively. This can be interpreted as due to the nanodarts being subjected only to electrostatic forces, whereas the cathode side nanotubes are subjected to the same forces but also to FE currents and related evaporation or destruction mechanisms.

Even more striking is Fig. 6 c) which shows the sample after 225 V (and 27 μA). All the remaining nanotubes protrude less than 300 nm into the gap. These small sizes do not prevent tube disappearance and self-oscillation induced destruction. On the other hand, the density of small emitters is greater than the density of long emitters at the beginning, which undoubtedly explains the stronger field emission currents obtained. Finally, at these voltages, we can even observe a disappearance of some nanodarts or at least the tearing off of the denditric branches observed previously. At these voltages the fields are extremely high and the fact that the nanodarts are a little bit longer proves their extremely robust contact with the support.

B. Destruction mechanisms during FE

1. *Uprooting and field evaporation*

Let's now discuss in more details the different destruction mechanisms observed during the FE experiments and that limit the field emission performances of CNT cathodes. As already discussed sudden destruction may be due to mechanical ripping-out of the nanotubes. Once again, a clear proof is given by Figs. 6 a) and b) with the formation of numerous nanodarts and their multiple branches. The second mechanism, also previously discussed, is the gradual destruction of the CNTs due to FE induced thermal field evaporation process. For example during the first I(V), presented in Fig. 5 a), two long nanotubes being gradually evaporated are observed. This limiting mechanism could be interesting for the field emission performances of CNT cathode since these gradual destructions can preserve the CNT for FE. This limitation effect could optimally equalize the initially broad field amplification factor distribution. This would lead to numerous CNTs with close amplification factor and rapid variation of the emission current. However we observed that this mechanism is often followed by total or partial destruction. To preserve a maximum number of these evaporating nanotubes, a slow voltage ramp during the initial voltage could be an appropriate treatment.

2. *Self oscillation induced destruction mechanism*

Finally the new destruction mechanism for field emitting SWNTs observed in the experiments is FE induced mechanical self-oscillations. In Fig. 4 b) and the corresponding film SM-video2, the nanotube labelled "2" presents an example of this destruction mechanism during FE. Another example is provided in SM-video3[17] from which the images a) to e) of the figure 8 are extracted. In this video one first observes that the nanotube goes in and out of self-oscillation, and then the self-oscillations are sustained but not very stable with the amplitude varying rapidly in time. In the last part, the tube seems to disappear during a few frames and finally only a small part

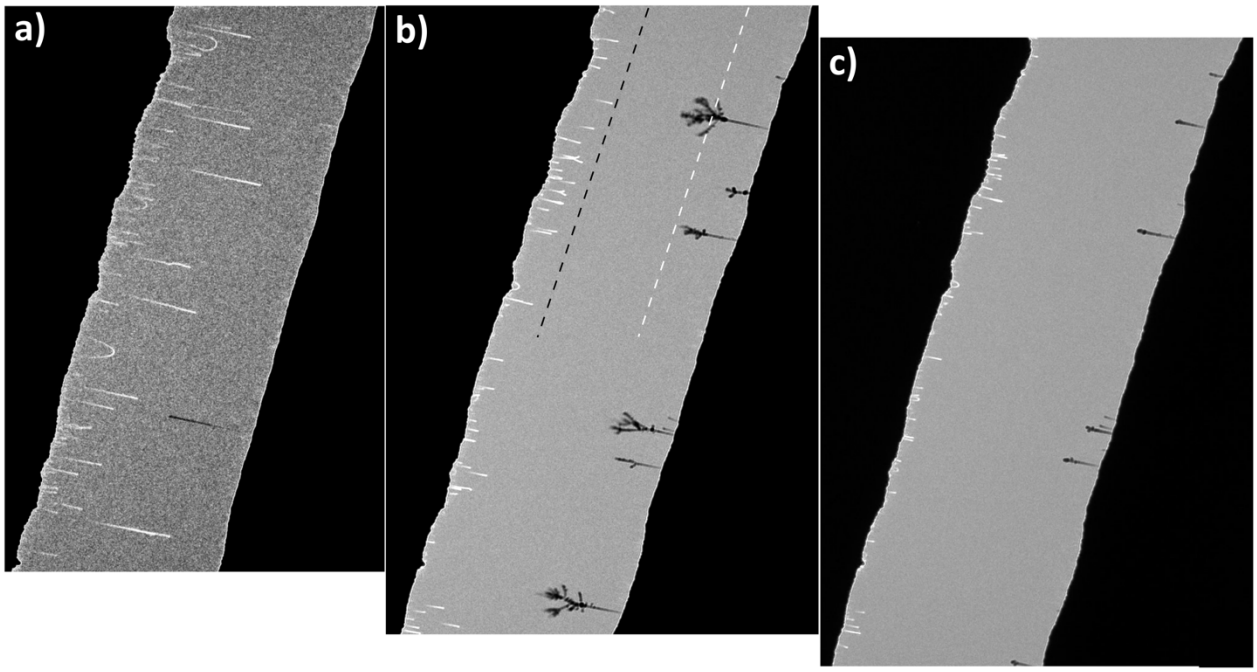

FIG. 6. Evolution of another cathode at different stages of the experiment. a) Image of the cathode at the end of the synthesis. Here the synthesis was shorter in order to avoid the formation of a foam at the base and the appearance of too many nanodarts. b) Image of the cathode after application of 125 V. We observe a shortening of the tubes and the appearance of nanodarts. The dotted lines represent the average lengths of nanotubes and nanodarts in the gap. c) Image of the sample after application of 215 V and an emission current of 27 μA. The nanotubes have been strongly shortened again and some nanodarts have disappeared.

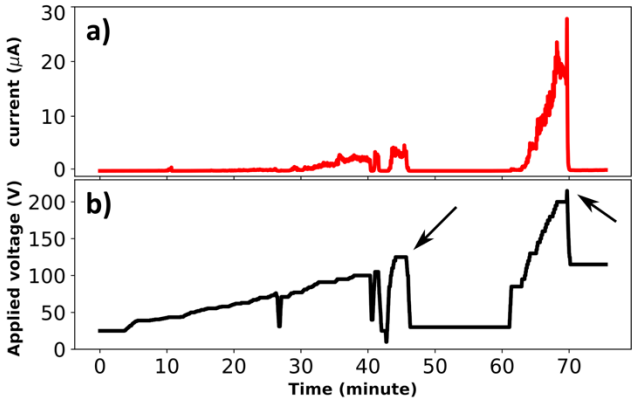

FIG. 7. a) Current evolution and b) applied voltage evolution for the sample presented in Fig. 6. The maximum current obtained corresponds to 27.8 μA for a voltage of 225 V. The correspondence with the images in Figs. 6 b) and c) is indicated by the two arrows.

of the nanotube remains, suggesting partial destruction. The apparent disappearance of the nanotube before destruction is due to very large oscillation amplitudes. Images Figs. 8 a) to e) show the last 5 frames before destruction and one can perceive in c) and d) the large oscillation envelope that is illustrated by the red arrow in c). These large amplitudes lead even to oscillations of nearby nanotubes.

Other characteristics of this self-oscillation destruction mechanism are : i) Self-oscillations generally appear close to the mechanical eigenmodes, with frequencies and oscillation shapes close to the natural frequencies and shapes. In videos, the most frequently observed case corresponds to the first mechanical eigenmode, but several self-oscillating tubes are also observed in the second eigenmode as shown in Figs. 8 f) to h) with the vibration node clearly visible. ii) This destruction mechanism is not limited to long nanotubes. Self-oscillation destructions have also been observed for short nanotubes. This phenomenon is then not simply related to the presence of nanodarts on the counter electrode. iii) This destruction mechanism contributes significantly to the loss of nanotubes of between 10 and 20 % of cases.

To our knowledge it is the first time that FE self-oscillations are reported to contribute significantly to nanotube destruction. Self-oscillation of emitting carbon nanotubes have already been reported in a few cases. Saito *et al.* observed in TEM strong oscillations of a bundle of SWNTs, glued at the apex on a tungsten tip by an electrophoresis technique, followed by a shortening of the bundle[22]. Self-oscillations have also been observed in totally different geometries for an individual MWNT[23] or on SWNTs membranes[24] but their geometry dependent self-oscillation mechanisms differ significantly from our cathode configuration. The fact that a self-oscillation mechanism is responsible for the notable destruction of SWNTs during FE is therefore highly original and raises several questions: Why has this mechanism not been clearly observed previously, what is the mechanism leading to

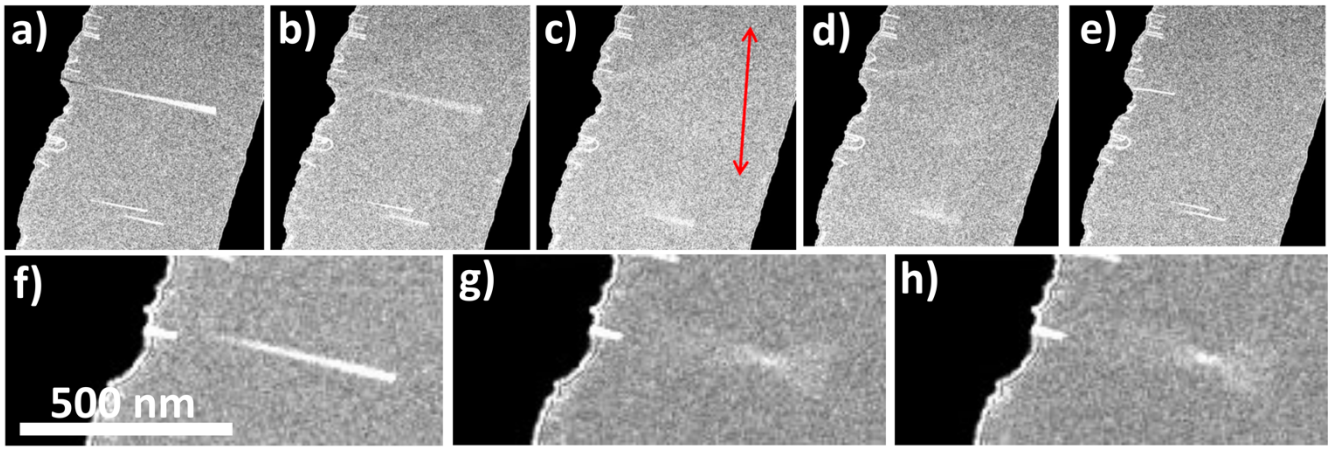

FIG. 8. Observation of the self-oscillation induced destruction mechanism. a) to e) The five last images of a self-oscillating nanotube before partial destruction. In c) and d) the nanotube is hardly visible due to very large oscillation amplitudes. The amplitude is illustrated by the red arrow in c). f) to h) another example of self-oscillations. In this case, the nanotube self-oscillates near the second mechanical eigenmode. The vibration node is almost the unique visible point of the nanotube.

these self-oscillations, and how can one possibly limit these self-oscillations to improve the cathode's performance?

Fundamental studies on individual SWNTs with good electrical contact in FEM configuration, such as presented by Dean *et al.*[11], did not report any observation of self oscillations although this phenomenon would have been easily detected in the FEM patterns. However, self-oscillations have previously been observed during FE for example on SiC nanowires[25,26] or diamond nanoneedles[27]. In these cases, it has been demonstrated that the self-oscillations were related to the electrical resistance of the nanowires. More precisely, the electrical potential at the apex, and hence the electrostatic forces, depends on the FE current which in turn depends on the field amplification factor which itself depends on the apex position. This creates a coupling between the mechanical degrees of freedom and the field emission current which can cause the appearance of self-oscillations. Typically, for SiC nanowires, self-oscillations were observed for currents in the nA range and the estimated nanowire resistances were between $10^9 - 10^{11}$ Ohm. In the case of our SWNTs it seems that self oscillations occur at higher currents. For example in Fig. 5 a) the current jump labelled "2", corresponding to a 500 nA drop, is related to the self-oscillation induced destruction of the nanotube labelled "2" in Fig. 4 b). As a consequence we propose that these self-oscillations may originate from the high contact resistance that can appear between CNT/catalyst/Alumina/Si heater. For a contact resistance of 1 MΩ and an emission current of 500 nA this leads to a voltage drop of 0.5 V that is perhaps sufficient to couple efficiently the FE and mechanical degrees of freedom. Further investigations are needed to confirm this hypothesis such as electron spectroscopy that allows the voltage drop due to a resistive effect to be measured[13].

Another question is why the self oscillations lead to the total or partial destruction of the CNT. For SiC nanowires, if some nanowires have been destroyed during self oscillations, the majority of the nanowires could self oscillate for weeks without destruction. This destruction cannot be due to a current runaway : in our diode configuration the oscillation moves the apex away from the anode, reducing the amplification factor. Oscillation then induce an AC current component at twice the mechanical resonant frequency and a reduction in the average emission current. Another possibility is that the large oscillation amplitudes can lead to nanotube fatigue and their eventual rupture. One can also imagine that the nanotube extremity sticks to a neighbouring one or to the support due to very large amplitudes or kink formation along the tube. These mechanisms, which require very large amplitudes, are supported by experimental observations which show that such amplitudes are obtainable. Indeed, at the beginning of the self-oscillation the amplitude grows exponentially. These are non-linear contributions which, if dissipative, can limit the amplitude and lead to a limit cycle. From a temporal point of view, if a self-oscillation were to start without non linear limitation, we would probably observe nothing. As the video frame rate is 4 Hz and the oscillation frequencies are in the 100 MHz range, from one frame to the next the tube would have acquired so much energy that the amplitude would result in it touching the support where it would remain attached. In video this would only correspond to a tube disappearing between frames.

In order to limit this destructive mechanism, it is necessary to know precisely what causes self-oscillation. If the cause is indeed a contact resistance, it would be necessary to improve the electrical contact between the tube and the support, for example by finding a barrier layer that is less electrically insulating than the alumina used in our study. Note also that the poor vacuum and hence the unstable field emission currents are probable destabilising parameters for self-oscillations.

To conclude this section on self-oscillations we can summarize the main characteristics observed: i) self-oscillations have been observed on many SWNTs. ii) their amplitude can be very large, iii) these self-oscillations lead more or less rapidly to nanotube destruction. It has to be confirmed whether this

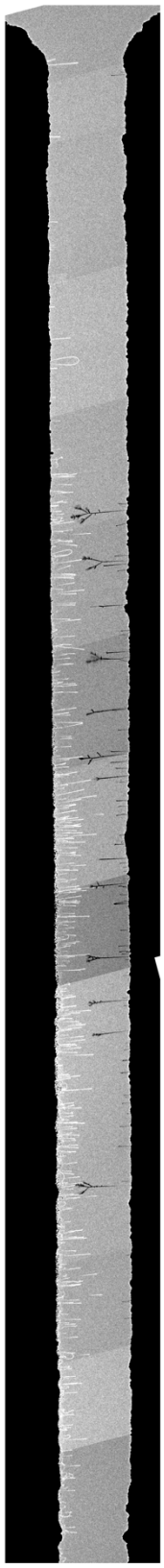

FIG. 9. Composite image of the gap during the synthesis presented in Fig. 1 c) and d). It can be seen that the synthesis is not uniform on the upper cantilever part probably due to a thermal gradient. The emitting zone can be estimated to be 100 μm^2.

destruction mechanism is common or not in nanotube field emission cathodes and to confirm the origin of these self-oscillations: contact resistance or another mechanism. It could also be interesting to "stabilize" this self-oscillation regime to obtain high-frequency AC current sources.

C. Current densities

Now considering the cathode as a whole, it is interesting to estimate the current densities obtained. A composite image of the synthesis zone for the sample presented in Fig. 1 c) and d) during growth is presented in Fig. 9. It can be seen that the synthesis is not uniform along the heated electrode. We can estimate the length of the sample where nanotubes can participate to emission to be 25 μm for a depth of 4 μm. This leads to an effective emitting surface of nearly 100 μm^2. At the time the picture has been taken the number of nanotubes longer than 500 nm in the gap can be estimated to be a little greater than 100. If the nanotubes were evenly distributed it would give one nanotube in a square of side 1 μm that would limit the mutual screening of the emitters. Our samples therefore lie in the gap between individual emitters and macroscopic cathodes with tens of thousands of emitters. Although it is extremely hazardous to extrapolate current density from small samples to larger cathodes we can however make some estimations. Considering an emission current of 2 μA for the first sample (see Fig. 2 a) and I(V) in Fig. 5 a)) and the maximum current of 27 μA for the second presented sample (see Fig. 7) and for an emission surface of 100 μm^2 this leads to a current density of 2 A/cm^2 and 27 A/cm^2 respectively that is rather good for non-optimised FE cathodes. This shows the possible interest of electric field-directed synthesis of SWNT for FE applications although experiments on larger surfaces will need to be done to confirm these values.

IV. CONCLUSION

In summary, we have shown the interest and unique possibilities of *in situ* observations under environmental TEM for the electric field-directed growth of single-walled nanotubes, and the evolution of nanotubes during field emission. Regarding growth, the application of an electric field enables highly effective alignment of the finest nanotubes, which holds great promise for field emission applications. In our samples, a significant part of the nanotubes are pulled out of the electrode and some of them attach firmly in the opposite electrode forming nanodarts which are also aligned by the electric field. For high fields the growth of the nanotubes can even be limited by the field emission and the thermally activated field evaporation phenomenon. The field emission measurements after synthesis allow us to observe the evolution of the nanotubes during the measurements as well as the destruction mechanisms. These mechanisms can be associated with nanotube tearing, gradual destruction via evaporation, and, in a more unique observation, a self-oscillation phenomenon that precedes the destruction. We propose that this self-oscillation

is related to the contact resistance between the nanotube and the electrode. It has to be confirmed whether this destruction mechanism is common or not in nanotube field emission cathodes and to confirm the origin of these self-oscillations. Our observations show that an important step would be to improve the mechanical contact between the nanotubes and the electrode by, for example, using an optimized barrier layer and catalyst, which would give better control of the density of emitting nanotubes and improve the current densities obtained which vary between 2 and 27 A/cm^2. More generally, the developed methodology and experimental setup allows an unprecedented access to the growth processes of highest quality CNTs, *in situ* post-growth modification and eventually to the metrology of a wide spectrum of their physical properties.

ACKNOWLEDGMENTS

Authors acknowledge financial support from the French state managed by the National Research Agency through the projects NanoMAX (ANR-10-EQPX-50), 3DRX ONline(ANR-15-CE08-0002) and Solitube (ANR-22-CE09-0005). The authors thank the Centre Interdiscipinaire de Microscopie Electronique de l'Ecole Polytechnique (CIMEX), the Plateforme Nanofils et Nanotubes Lyonnaise of the University Lyon and the METSA (Microscopie Electronique et Sonde Atomique) network.

AUTHOR DECLARATIONS

Conflict of Interest

The authors have no conflicts to disclose

DATA AVAILABILITY

The data that support the findings of this study are available from the corresponding author upon reasonable request.

[1]Y. Saito (Editor), *Nanostructured Carbon Electron Emitters and Their Applications* (CRC Press, 2022).
[2]C. Huo, F. Liang, and A. Sun, "Review on development of carbon nanotube field emission cathode for space propulsion systems," High Voltage **5**, 409–415 (2020).
[3]R. Parmee, C. Collins, W. Milne, and M. Cole, "X-ray generation using carbon nanotubes," Nano Convergence **2**, 1 (2015).
[4]D. Spronk, Y. Luo, C. Inscoe, Y. Lee, J. Lu, and O. Zhou, "Evaluation of carbon nanotube x-ray source array for stationary head computed tomography," Medical Physics **48**, 1089–1099 (2015).
[5]C. Puett, C. Inscoe, A. Hartman, J. Calliste, D. Franceshi, J. Lu, O. Zhou, and Y. Lee, "An update on carbon nanotube-enabled x-ray sources for biomedical imaging," Advanced Review **10**, e1475 (2017).
[6]F. Houdellier, L. de Knoop, C. Gatel, A. Masseboeuf, S. Mamishin, Y. Taniguchi, M. Delmas, M. Monthioux, M. Hytch, and E. Snoeck, "Development of tem and sem high brightness electron guns using cold-field emission from a carbon nanotip," Ultramicroscopy **151**, 107–115 (2015).
[7]P. Legagneux, P. Guiset, N. Le Sech, J. Schnell, L. Gangloff, W. Milne, C. Cojocaru, and D. Pribat, "Microwave amplifiers," (in Carbon Nanotube and Related Field Emitters, Wiley-VCH, 2010) Chapter 27, pp. 439–468.
[8]J. Zhang, C. J., J. Xu, Q. Wang, M. Sun, W. Zou, H. Xu, and X. Zhang, "Development of a k-band traveling wave tube based on carbon nanotube cold cathode," Vacuum **203**, 111231 (2022).
[9]B. Crossley, N. E. Glauvitz, B. Quinton, R. Coutu, and P. Collins, *"Characterizing Multi-Walled Carbon Nanotube Synthesis for Field Emission Applications," in Carbon nanotubes applications on electron devices/ monograph by Jose Mauricio Marulanda. Rijeka, Croatia : InTech* (2011).
[10]Y. E. Saito, *Carbon Nanotube and Related Field Emitters: Fundamentals and Applications. ISBN: 978-3-527-32734-8* (Wiley-VCH, 2010).
[11]K. Dean, T. Burgin, and B. Chalamala, "Evaporation of carbon nanotubes during electron field emission," Appl. Phys. Lett. **79**, 1873 (2001).
[12]M. Wang, Q. Chen, and L. Peng, "Field-emission characteristics of individual carbon nanotubes with a conical tip: The validity of the fowler–nordheim theory and maximum emission current," Small **4**, 1907 (2008).
[13]S. Purcell, P. Vincent, C. Journet, and V. Binh, "Hot nanotubes: Stable heating of individual multiwall carbon nanotubes to 2000 k induced by the field-emission current," Phys. Rev. Lett. **88**, 105502 (2002).
[14]J. Bonard, C. Klinke, K. Dean, and B. Coll, "Degradation and failure of carbon nanotube field emitters," Phys. Rev. B **67**, 115406 (2003).
[15]A. Pascale-Hamri, S. Perisanu, A. Derouet, C. Journet, P. Vincent, A. Ayari, and S. Purcell, "Ultrashort single-wall carbon nanotubes reveal field-emission coulomb blockade and highest electron-source brightness," Phys. Rev. Lett. **112**, 126805 (2014).
[16]P. Vincent, F. Panciera, I. Florea, N. Blanchard, C. Cojocaru, M. Ezzedine, H. Taoum, S. Perisanu, P. de Laharpe, A. Ayari, J. Chaste, K. Saidov, U. Mirsaidov, S. Purcell, and P. Legagneux, "Observations of the synthesis of straight single wall carbon nanotubes directed by electric fields in an environmental transmission electron microscope," Carbon **213**, 118272 (2023).
[17]See supplementary material at [URL will be inserted by AIP Publishing] for a short description of videos given as supplementary Materials.
[18]J. Buchoux, L. Bellon, S. Marsaudon, and J.-P. Aimé, "Carbon nanotubes adhesion and nanomechanical behavior from peeling force pectroscopy," Eur. Phys. J. B **84**, 69 (2011).
[19]T. Li, A. Ayari, and L. Bellon, "adhesion energy of single wall carbon nanotube loop on various susbstrates," J. Appl. Phys. **117**, 164309 (2015).
[20]R. Rosen, W. Simendinger, C. Debbault, H. Shimoda, L. Fleming, B. Stoner, and O. Zhou, "Application of carbon nanotubes as electrodes in gas discharge tubes," Appl. Phys. Lett. **76**, 1668 (2000).
[21]B. Liang, A. Ogino, and M. Nagatsu, "Discharge characteristics of a nano-sized electrode with aligned carbon anotubes grown on a tungsten whisker tip under various gas conditions," J. Phys. D : Appl. Phys. **43**, 275202 (2010).
[22]Y. Saito, K. Seko, and J. Kinoshita, "Dynamic behavior of carbon nanotube field emitterss observed by in situ transmission electron microscopy," Diamond and Related Materials **14**, 1843 (2005).
[23]J. Weldon, B. Aleman, A. Sussman, W. Gannett, and A. Zettl, "Sustained mechanical self-oscillations in carbon nanotubes," Nano Letters **10**, 1728 (2010).
[24]V. Kleshch, A. Obraztsov, and E. Obraztsova, "Electromechanical self-oscillations of carbon nanotube field emitter," Carbon **48**, 3895 (2010).
[25]A. Ayari, P. Vincent, S. Perisanu, M. Choueib, V. Gouttenoire, M. Bechelany, D. Cornu, and S. Purcell, "Self-oscillations in field emission nanowire mechanical resonators : a nanometric dc-ac conversion," Nanoletter **7**, 2252 (2007).
[26]A. Lazarus, E. de Langre, P. Manneville, P. Vincent, S. Perisanu, A. Ayari, and S. Purcell, "Statics and dynamics of a nanowire in field emission," International Journal of Mechanical Sciences **52**, 1396 (2010).
[27]V. Kleshch, R. Ismagilov, V. Mukhin, A. Orekhov, P. Poncharal, S. Purcell, and A. Obraztsov, "Electromechanical resonances and field-emission-induced self-oscillations of single crystal diamond needles," Appl. Phys. Lett. **122**, 144101 (2023).